frontiers | Frontiers in Earth Science

TYPE Original Research
PUBLISHED 09 November 2023
DOI 10.3389/feart.2023.1174504

OPEN ACCESS

EDITED BY
Marcelo Ketzer,
Linnaeus University, Sweden

REVIEWED BY
Shinsuke Aoki,
Kagawa University, Japan
Nadezhda Syrbu,
V.I. Il'ichev Pacific Oceanological Institute (RAS), Russia
Saulwood Lin,
National Taiwan University, Taiwan

*CORRESPONDENCE
Tomohiro Toki,
toki@sci.u-ryukyu.ac.jp

RECEIVED 26 February 2023
ACCEPTED 26 October 2023
PUBLISHED 09 November 2023

CITATION
Toki T, Chibana H, Shimabukuro T and Yamakawa Y (2023), Distribution of dissolved methane in seawater from the East China Sea to the Ryukyu forearc. *Front. Earth Sci.* 11:1174504. doi: 10.3389/feart.2023.1174504

Distribution of dissolved methane in seawater from the East China Sea to the Ryukyu forearc

Tomohiro Toki[1,2]*, Hideki Chibana[1], Teppei Shimabukuro[1] and Yo Yamakawa[1]

[1]Department of Chemistry, Biology and Marine Science, Faculty of Science, University of the Ryukyus, Nishihara, Okinawa, Japan, [2]Research Institute for Humanity and Nature, Kyoto, Japan

Methane is a greenhouse gas, and the East China Sea acts as a source of emissions to the atmosphere. On the other hand, the distribution of methane concentration in the Ryukyu Arc shelf and forearc region has not been clarified. Therefore, we investigated the continental slope and continental shelf areas from the Okinawa Trough to the landward side and the island shelf and forearc areas to the seaward side of the East China Sea. The methane concentration in the Kuroshio Current region was very low, and the methane concentration in the seawater just above the seafloor in the area directly above the hydrothermal systems was exceptionally high. In addition, methane concentration in seawater just above the seafloor where cold seeps and mud volcanoes are known is higher than the background, and higher methane concentrations were found in continental slope area and the island shelf area. The results suggest the existence of previously unreported methane sources such as cold seeps and mud volcanoes in the continental slope region and the island shelf region.

KEYWORDS

East China Sea, seawater, water column, methane, concentration, distribution, Ryukyu forearc

1 Introduction

Methane is a greenhouse gas that is estimated to be 80 times more potent than carbon dioxide over the next 20 years, making it extremely important to quantify the material cycle of the gas in the Earth's surface layer (Shukla et al., 2022). Continental shelves play extremely important roles as sources of the methane that is released into the atmosphere (Bange et al., 1994; Holmes et al., 2000; Bange, 2006). The methane that is stored in the stratified seawater of the East China Sea during summer is released into the atmosphere by the mixed layer that develops during winter (Tsurushima et al., 1996). Topographic features and gas chimneys that are presumed to be associated with mud volcanoes have been observed on the continental shelf and in the Okinawa Trough (Yin et al., 2003; Xing et al., 2016), together with cold seep sites on the continental slope (Xu et al., 2021), chemosynthetic organisms in the northern part of the Okinawa Trough (Kuhara et al., 2014; Xu et al., 2021), and exposed carbonate sites on the seafloor surface that suggest former cold-seep activity (Sun et al., 2015; Peng et al., 2017; Cao et al., 2020), all of which were potential sources of methane. Methane concentration anomalies and acoustic anomalies that suggest the presence of gas flares have been observed immediately above these sites, indicating that the cold-seep activity is ongoing (Zhang et al., 2020). These cold seep activities are considered related to the dissociation of methane hydrate (Sun et al., 2015; Cao et al., 2020), and are

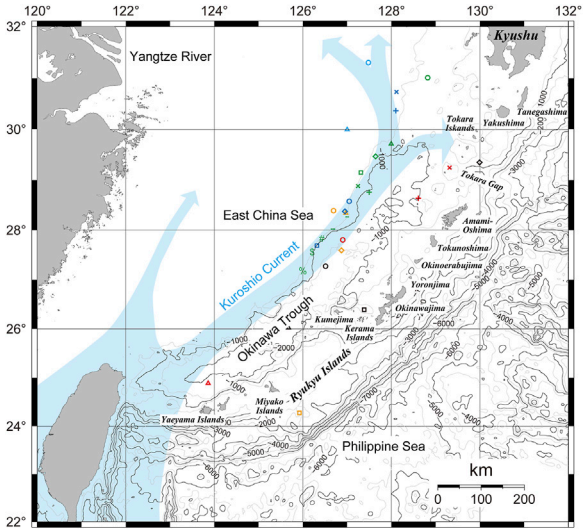

FIGURE 1
Location of sampling points and bathymetric map of the surrounding seas. Sampling points are indicated using the symbols shown in Table 1. Revisited sites are denoted using open symbols. Thin contour lines denote distances of 500 m and thick lines 1,000 m, and water depth is labeled every 1,000 m. The blue square and diamond indicate high methane concentrations in pore water found by the Chinese group (Li et al., 2015). Blue × and + indicate locations where the Chinese group found carbonate (×: Sun et al., 2015; +: Sun et al., 2019).

thought to have been one cause of the slope failure (blue × in Figure 1) and contributed to global warming that occurred after the last glacial period (Cao et al., 2020). Methane is rarely found in oxidizing seawater, and is abundant in methane-seeping phenomena on the seafloor, such as cold seeps, hydrothermal systems, and mud volcanoes, and river water of continental origin (Sun et al., 2018). For this reason, many studies have been conducted to discuss the supply source of methane to seawater by combining the T-S diagram, which combines water temperature and salinity, with the concentration distribution of methane (e.g., Zhang et al., 2020). In accordance with them, in this study, we investigated the concentration distribution of methane from the continental shelf of the East China Sea to the forearc region of the Ryukyu arc, and combined it with the T-S diagram to discuss the supply source of methane to seawater.

2 Methods

2.1 Sampling points

Seawater samples were collected aboard the Nagasaki Maru vessel during end of May to the beginning of June in 2010–2015 (Table 1; Figure 1). We took 303 samples (Figure 1). Sampling was conducted over the continental shelf, continental slope, the Okinawa Trough, island shelf, and forearc slope, which were classified in accordance with distance from the continent. The sites were selected such that each area had as many "featureless seafloor" combinations and singular geological points as possible. Henceforth in this paper, we refer to "featureless seafloor" as seafloor with no reported submarine hydrothermal systems, mud volcanoes, cold seeps, pockmarks, etc. The symbols used are summarized in Table 1, and the same symbols are used in all figures. The continental shelf is denoted yellow, continental slope is green, and sites further offshore are black. Mud volcanoes are indicated in brown, cold seeps in blue, and submarine hydrothermal systems in red. In the five revisited sites (Site No. 2015-3, 2012-1, 2015-5, 2012-7, and 2012-8), data from the first visit are indicated by open symbols, and data from the second by solid symbols. Only the open symbols are utilized on the map (Figure 1). Continental slope data were collected from a large number of points located in the same study area; therefore, this feature was divided into north and south with a boundary lying at approximately 28°30′N.

2.2 Seawater sampling

Niskin samplers were used to collect seawater, and CTD sensors utilized to simultaneously measure water temperature, pressure, and salinity. Once at the designated location, the water sampler was lowered to the area just above the seafloor, and seawater was sampled at the designated depth using the water sampler with a 12-hanger. Sampling was conducted according to depth, and a bucket was used to obtain surface samples. Seawater samples were divided into two vials and 500 µL of saturated mercury solution immediately added to inhibit the microbial activity. Samples were then capped with a butyl rubber stopper and aluminum cap and stored around 4 °C in a refrigerator to prevent rupture before transfer to a laboratory refrigerator for analysis.

2.3 Analytical procedures

Dissolved gases were extracted from 100 mL samples of seawater and measured using a gas chromatograph equipped with an FID (GC-2014; Shimadzu, Supplementary Figure S1). The samples (100 mL) were transferred to a purge bottle using helium gas and helium bubbling initiated until almost all dissolved gas reached the gas-phase. Initial water vapor removal was performed by passing gas through a cold trap that was cooled at −120 to −80°C using liquid nitrogen and ethanol, after which gas was filtered through silica gel at room temperature for further water vapor removal. The six-way valve was used to allow carrier gas to flow out of the gas chromatograph, and all trapped gas was vaporized with boiling water. The degassed sample was then placed in the gas chromatograph, separated by a Porapak Q column, and carried into the FID detector, where all gases were burned and ionized to measure the concentration of hydrocarbons. The standard gas was introduced upstream of a bottle filled with ultrapure water, after ensuring that the blank containing 10 ppm methane was completely lowered at a measured pressure. Gas extracted using a similar method was analyzed by FID to determine the sensitivity for methane. Analysis was performed until the accuracy reached less than 8%. The same seawater sample was measured daily to ensure that the concentrations were within the error limit of 8% before the sample was measured. Sample weights were calculated by weighing

10.3389/feart.2023.1174504

TABLE 1 Location and description of seawater sampling by a Niskin sampler.

Location	Area	Site no.	Year	Month	Symbol	Longtitude	Latitude	Depth (m)	Remarks
Continental shelf		2011-6	2011	May	○	127°28.899′E	31°18.042′N	127	
		2011-5	2011	May	△	127°00.020′E	29°59.945′N	105	
		2012-3	2012	May	○	126°41.336′E	28°22.234′N	186	Mud volcano Yin et al. (2003)
Continental slope	Northern area	2011-7	2011	May	○	128°49.805′E	31°00.336′N	679	
		2015-1	2015	June	△	127°59.916′E	29°43.132′N	726	
		2015-2	2015	June	◇	127°38.223′E	29°27.710′N	821	
		2011-4	2011	May	□	127°20.055′E	29°08.207′N	601	
		2015-3	2015	June	■	127°19.910′E	29°08.175′N	595	Revisit to Site 2011-4
		2015-4	2015	June	×	127°15.16′E	28°51.70′N	778	
		2011-3	2011	May	+	127°30.092′E	28°44.832′N	1,027	
		2012-1	2012	June	⊞	127°30.250′E	28°44.996′N	1,025	Revisit to Site 2011-3
		2012-2	2012	May	○	127°02.830′E	28°33.655′N	648	Cold seep Kuhara et al. (2014)
		2015-5	2015	May	●	127°02.944′E	28°33.811′N	655	Revisit to Site 2012-2
	Southern area	2015-6	2015	May	-	127°00.149′E	28°13.636′N	864	
		2015-7	2015	May	−	126°40.30′E	28°00.544′N	710	
		2015-8	2015	May	#	126°25.576′E	27°48.572′N	1,024	
		2015-9	2015	May	$	126°12.513′E	27°33.070′N	970	
		2015-10	2015	May	%	125°59.65′E	27°10.32′N	1,024	
		2012-4	2012	May	△	126°58.176′E	28°19.612′N	431	Pockmark Yin et al. (2003)
Backarc area		2011-1	2011	May	○	126°30.185′E	27°14.869′N	1,554	Control site 1
		2012-7	2012	May	●	126°30.507′E	27°15.182′N	1,563	Revisit to Site 2011-1
		2010-1	2010	May	△	125°40.132′E	26°00.202′N	1,889	
		2012-5	2012	May	◇	126°52.314′E	27°34.298′N	1,478	Mud volcano Ning et al. (2009)
		2012-6	2012	May	○	126°54.021′E	27°47.318′N	1,835	Iheya North Knoll Monma et al. (1996)
		2010-2	2010	May	△	123°50.992′E	24°51.661′N	1,596	Hatoma Knoll Watanabe et al. (1999)

(Continued on following page)

TABLE 1 (*Continued*) **Location and description of seawater sampling by a Niskin sampler.**

Location	Area	Site no.	Year	Month	Symbol	Longtitude	Latitude	Depth (m)	Remarks
Island shelf		2011-8	2011	May	◇	129°59.865′E	29°20.105′N	1,134	
		2011-2	2011	May	□	127°23.007′E	26°22.095′N	748	
		2012-8	2012	May	■	127°23.053′E	26°22.174′N	746	Revisit to Site 2011-2
Forearc slope		2010-3	2010	May	□	125°55.135′E	24°15.067′N	1,385	Potential mud volcano

each tare and subtracting the average weights of the empty bottle, butyl rubber stopper, and aluminum cap. The concentration of each sample (M) was then calculated as the concentration of methane per kilogram of seawater (mol/kg).

3 Results

3.1 T-S diagram

The salinity and temperature data obtained from the CTD were used to produce a T-S diagram with salinity on the horizontal axis and temperature on the vertical axis (Figure 2). Kuroshio Surface Seawater (KSW), Kuroshio Sub-surface Seawater (KSSW), Kuroshio Intermediate Seawater (KIW), and Shelf mixed seawater (SMW) are identified in all water masses (Zhang et al., 2008). Graphs were divided into different sea areas and "geological singularities" (Figure 2). Henceforth in this paper, submarine hydrothermal systems, mud volcanoes, cold seeps, and pockmarks are referred to as geologic singularities. Figures 2A–C shows the salinity and temperature data describing seawater collected from the featureless seafloor of the continental shelf (Site No. 2011–6, 2011–5, and 2012–3). Among them, Figure 2C is the CTD data acquired over the mud volcanic landform reported by Yin et al. (2003). Figures 2D–M shows the northern part of the continental slope, Figures 2L, M shows the cold seep site reported at the southern end of the northern continental slope (Kuhara et al., 2014), and Figures 2N–S shows the T-S data acquired from the southern part of the continental slope, and Figure 2S shows data collected over the pockmarks reported by Yin et al. (2003). Figures 2T–Y shows the T-S data from above the Okinawa Trough, Figure 2W shows data acquired from above the mud volcanoes (Ning et al., 2009) reported in the Okinawa Trough, and Figures 2X, Y shows the T-S data obtained from the area above the submarine hydrothermal system corresponding to the geological singularity in the Okinawa Trough. Figures 2Z–ab shows the data acquired from the area above the island shelf, and Figure 2ac illustrates the data acquired from the forearc region.

The T-S data obtained from the top of the featureless seafloor of the Okinawa Trough are considered representative of the Kuroshio Current (Figures 2T–V), and the inverse S-shaped curve from the KSW to the KIW via the KSSW is typical of that obtained using T-S data for water masses in the Kuroshio Current (Figures 2T–V). Data from water masses above the continental shelf are mostly outside these regions and curves, and are interpreted to be continental shelf mixed water (SMW) (Figures 2A–C). The surface water above the continental shelf is cooler and less saline than that of the KSW (Figures 2A–C). Ultimately, continental river water is considered to be the end member; however, because it is river water, its salinity is lower than that of seawater, and its water temperature is also lower than that of warmer currents such as the Kuroshio Current. The influence of the SMW is clearly visible in the water masses above the continental shelf (Figures 2A–C, but it is also visible in some of the water masses in the continental slope region, especially the northern waters (Figures 2D–I). Similarly, the influence of the SMW is visible in the water masses above the cold-seep site classified as the northern sea area, especially in 2012 (Figure 2L). The fact that this is not as evident in the 2015 data (Figure 2M) suggests differences in water mass between 2012 and 2015. However, the SMW influence was relatively small in the data from 2015-6, 2015-7, 2015-8, 2015-9, and 2015-10 at sites south of 28°30′N and above the pockmark (site 2012-4), which are classified as the southern area (Figures 2N–S). The data obtained from the seafloor hydrothermal system on the island shelf and in the forearc slope region are plotted within the KSW, KSSW, and KIW (Figures 2T–ab). Only data from the slope area of the forearc deviated slightly from the KIW region, possibly because it was not a Kuroshio Current region in the first place (Figure 2ac). In any case, the T-S diagram generally shows the strong influence of continental shelf mixed waters on the continental shelf and in the northern part of the continental slope area, but not in other areas, and geological features such as submarine hydrothermal or mud volcanoes do not seem to influence the T-S diagram (Figure 2). The T-S is thus considered to be controlled mainly by factors such as ocean area, distance from the continent, and the influence of the meandering Kuroshio Current or continental rivers at shallower than about 100 m.

3.2 Vertical distribution of methane concentration

The distribution of methane concentrations was divided in the same manner as the CTD data (Figure 3). Classification was categorized into continental shelf (Figures 3A–C), northern continental slope (Figures 3D–K), the cold seep located at the southern end of the northern continental slope (Figures 3L, M), southern continental slope (Figures 3N–S), Okinawa Trough (Figures 3T–W), submarine hydrothermal system located in the Okinawa Trough (Figures 3X, Y), island shelf (Figures 3Z–ab), and mud volcano-like features in the forearc slope area (Figure 3ac).

10.3389/feart.2023.1174504

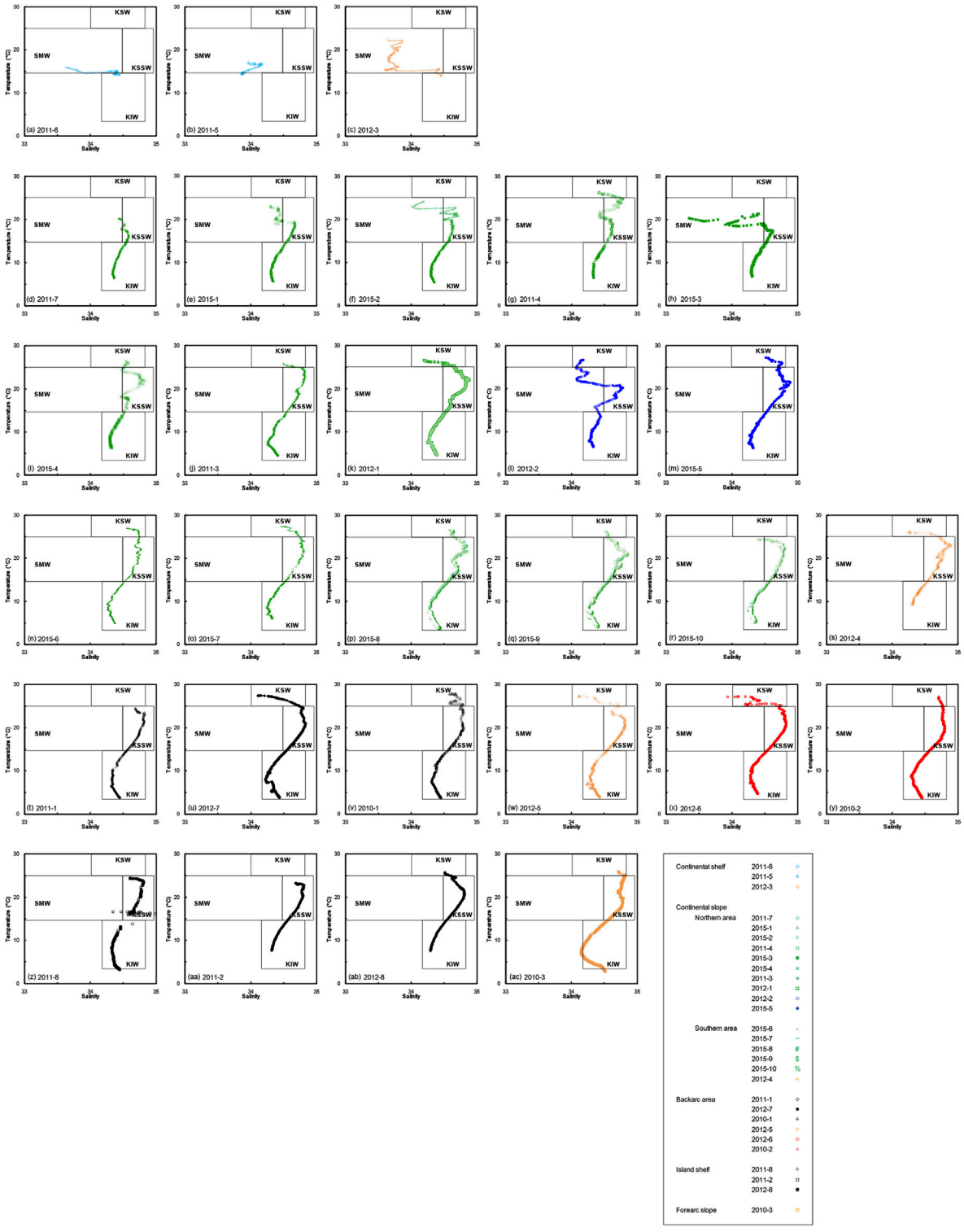

FIGURE 2
T-S diagram for sampling stations in the study. KSW, Kuroshio Surface Water; KSSW, Kuroshio Subsurface Water; KIW: Kuroshio Intermediate Water; SMW, the Shelf Mixed Water in the ECS. Water masses are classified according to Zhang et al. (2008). Light blue symbols indicate samples collected from the continental shelf **(A,B)**, green indicates samples collected above the continental slope **(D–K)**, **(N–R)**, and black denotes samples collected from other areas **(T–V)**, **(Z–ab)**. Samples collected directly above mud volcanoes are in orange **(C, S, W, and ac)**, samples collected just above the cold seep site are in blue **(L,M)**, and samples collected just above the hydrothermal system are in red **(X,Y)**. The high number of sampling points on the continental slope area led to division of this feature into northern **(D–K)** and southern **(N–R)** regions with the boundary at around 28°30′N latitude.

10.3389/feart.2023.1174504

FIGURE 3
Vertical distribution of methane concentrations in seawater obtained in this study. Symbols and groupings are the same as in Figure 2. Shading indicates background levels in seawater certified with reference to data from site 2017-7 **(U)** (see Section 3.2).

Classification is based on submarine morphology such as continental shelf, continental slope, back-arc basin (Okinawa Trough), forearc uplift zone (island shelf), and forearc trench side slope, which changes significantly with distance from the continent, and by the presence of as geological features such as submarine hydrothermal systems, cold seeps, and mud volcanoes (both reported and potential). Each site is plotted on a different graph. The colors and shapes of the symbols used are listed in Table 1.

First, we examine the distribution of methane concentrations in seawater collected from the area over Okinawa Trough (Figures

3T–V). This area could have ocean water without continental influence as the distribution of methane, because it is part of the Kuroshio Current region. According to these data, the methane concentrations in the seawater were one to two nM up to 400 m below the surface and 0–1 nM at greater depths (Figure 3U). These methane concentration distributions are shown as shaded areas in all graphs in Figure 3, as they correspond to the background of this area.

The distribution of methane concentrations in seawater collected over the continental shelf reveals slightly higher methane concentrations (Figures 3A, B), albeit with small differences, even on a featureless seafloor. On the other hand, the methane concentration in the seawater sampled above a mud volcano (Yin et al., 2003) on the continental shelf (Figure 3C) indicated that the methane concentration was within the same range as the background in the surface layer and increased rapidly below 100 m depth, with a maximum concentration observed at 120 m, below which it dropped. However, a particularly large peak of 10–12 nM was observed at approximately 150 m, and the methane concentration decreased to almost background levels immediately above the seafloor (Figure 3C).

Next, we examined the distribution of methane concentrations in seawater collected from the continental slope region (Figures 3D–S). According to these results, methane concentrations appear to be somewhat scattered in the southern region (Figures 3N–S) but are mostly within the range of background methane concentrations (note that the other graphs have different concentration ranges), including seawater above the pockmarked topography on the continental slope reported by Yin et al. (2003) (Figure 3S). In addition, the distribution of methane concentrations in the seawater just above the cold-seep site, where sampling was conducted twice (Figures 3L, M), shows much higher methane concentrations (~4 nM) over the surface 100–200 m (Figure 3L) than the background (shaded area in Figure 3L). The methane concentration decreases at 300 m, increases at 400 m, decreases again at 500 m, and increases just above the seafloor. However, in the seawater sampled during the return visit in 2015 (Figure 3M), the methane concentration anomaly observed at around 200 m was not observed, with only the increase just above the seafloor observed. In comparison, methane concentrations in the northern part of the continental slope were generally high (Figures 3D–K) and were significantly higher than the background at approximately 100–200 m below the surface at most sites. Methane concentrations reaching far above background levels were observed at depths below 400 m at several of the sites, with relatively large concentrations observed just above the seafloor at Site No. 2012-1 (Figure 3K). This site was also visited in 2011, the year before the concentration anomaly was observed (Figure 3I), and although the methane concentration at that time was not as high, a peak was observed in the seawater at 800 m (approximately 200 m above the seafloor), similar to 2012 (Figure 3I).

The methane concentrations in seawater sampled above the submarine hydrothermal systems were exceptionally high (Figures 3X, Y). High concentrations of >10 nM were obtained from seawater above known mud volcanoes on the continental shelf (Figure 3C) and in methane-rich seawater on the continental slope (Figure 3G). In contrast, methane concentrations in seawater collected above the seafloor hydrothermal system at the Iheya North Knoll (Figure 3X) exceeded 30 nM, although methane concentrations of only slightly above 10 nM were obtained above the Hatoma Knoll (Figure 3Y).

Site No. 2011-2, an island shelf area (Figure 3aa), was revisited in 2012 (Figure 3ab) and methane above background levels was detected in the samples taken during the second visit in 2012. The concentration distribution of methane in the seawater collected during the first visit in 2011 (Figure 3aa) was similar in shape to that in 2012; however, the absolute value of concentration was approximately 30% lower. Methane concentrations in seawater up to 200 m below the surface remained at background levels in 2011 (Figure 3Z) but were slightly higher than the background in the water mass at 300–500 m. Site No. 2011-8 (Figure 3Z) is located on the same island shelf; however, it is much farther north than the other island shelf sites and is situated in the Tokara Gap, which connects the Okinawa Trough to the Philippine Sea (Figure 1). The methane concentration distribution at Site No. 2011-8 (Figure 3Z) shows background levels in the surface layer with mild methane concentration anomalies in water masses below 400 m in depth.

Finally, the distribution of methane concentrations in the seawater sampled over the volcano-like mud terrain in the forearc region showed methane concentrations at background levels (Figure 3ac).

4 Discussion

4.1 Background concentration distribution of methane in seawater

Let us define the normal distribution of methane in seawater. In the surface layer of the ocean, the concentration is approximately 1–2 nM, which decreases to an extremely low concentration of 0–1 nM at depths below 400 m (Figure 3U). This suggests that methane reaches a solubility equilibrium with the atmosphere in the surface layer and is oxidized by microorganisms in the water column at depths below 400 m, resulting in the low concentrations observed. Methane is also produced by the decomposition of organic matter in the sediments, from which it can seep, resulting in high methane concentrations both in the sediments and in the seawater just above the seafloor (Sun et al., 2018). In some locations, the methane concentrations in the seawater immediately above the seafloor are particularly high because of disturbance to the seafloor surface, such as that observed in shallow waters under the action of strong currents or in areas with discharging fluids such as hydrothermal or cold-seep fluids (Zhang et al., 2020). Even at these locations, methane in the seawater is degraded by methane-oxidizing microorganisms away from the seafloor, and methane concentrations in the mid-water drop to very low concentrations of 0–1 nM (Watanabe et al., 1995).

4.2 The Yangtze River as a source of methane

The distribution of methane in seawater above the continental shelf is characterized by 1) low salinity and high methane concentration, mainly in the ocean surface layer at the mouth of

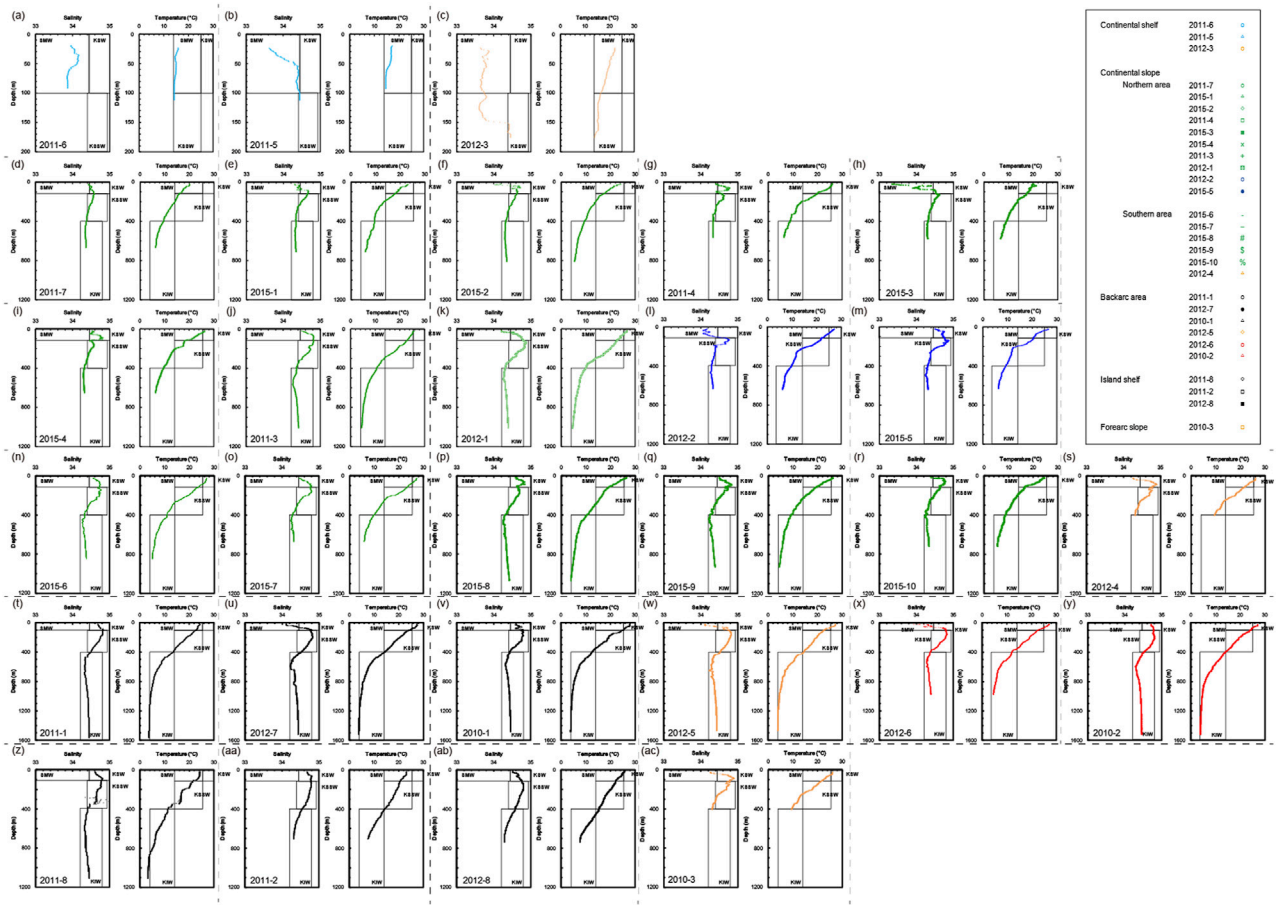

FIGURE 4
Vertical profiles of salinity and water temperature at the grouped stations. Symbols and groupings are the same as in Figure 2. The areas of each water mass are indicated by squares using water temperature and salinity data from Zhang et al. (2008).

the Yangtze River, and 2) high methane concentrations just above the seafloor due to the release of methane from the sediments (Sun et al., 2018). In this study, the effects of SMW mixing with low-salinity water of riverine origin were observed on the continental shelf (Figures 2A, B) and continental slope areas (Figures 2D–M). To verify whether these influences also affect the methane concentrations in ocean water, we plotted the distributions of salinity and temperature with depth (Figure 4). As before, the graphs were divided into the continental shelf (Figures 4A–C), northern part of the continental slope (Figures 4D–K), cold seep site located in the northern part of the continental slope (Figures 4L, M), southern part of the continental slope (Figures 4N–S), Okinawa Trough (Figures 4T–W), submarine hydrothermal system in the Okinawa Trough (Figures 4X, Y), and the island shelf area (Figures 4z–ab). The colors and shapes of the symbols used are the same as those listed in Table 1. The water temperature and salinity characteristics for each water mass shown in Figure 2 are boxed in accordance with depth, with water depths shallower than 100 m considered KSW, water between 100 and 400 m denoted KSSW, and water masses deeper than 400 m characteristic of KIW (Zhang et al., 2008). No distribution of the water masses was observed outside the KIW at any of the sites, and no middle water other than that of Kuroshio origin was found. In contrast, water masses with lower salinity (≤34–34.45 psu) and temperatures (≤25 C) than KSW are distributed in water at depths shallower than 100 m (Figures 4A–M).

The water sampled on the continental shelf, which is only approximately 100 m deep, shows lower salinity and temperature than the KSW (Figures 4A, B), suggesting that it is influenced by water of riverine origin (SMW in Figures 4A, B). The methane concentrations on the continental shelf show modest anomalies (~two to three nM) that are only slightly higher than the background (~1–1.5 nM; Figures 3A, B). This suggests that SMW is characterized by a methane concentration anomaly of only a few nM.

Seawater was also sampled just above the mud volcanoes on the continental shelf (Figure 3C), where the salinity is uniformly low (<34.5 psu) from the surface to a depth of approximately 150 m (Figure 4C), suggesting that low-salinity water of riverine origin may be influential in this area. Salinity was observed to increase sharply from ~33.7–33.8 psu to ~34.4 psu and water temperature decrease slightly around 15°C with depth in this location (Figure 4C), indicating that the KSSW can affect depths below 150 m (Figure 4C). In contrast, the methane concentration increases sharply at a depth of approximately 100 m, decreases at around 130 m, and reaches a maximum between 140 and 160 m (Figure 3C). Continental water originally contains a large amount of methane

TABLE 2 Maximum concentrations of methane in seawater immediately above the hydrothermal system in the Iheya North and Hatoma Knoll obtained in this study and reported end-membered concentrations of methane in hydrothermal fluid. In addition, similar datasets reported for the Okinawa Trough and representative similar datasets for other areas are also presented for comparison.

		Endmembered CH_4	Plume CH_4	References
		mM	nM	
Iheya North Knoll		3.7	30	Kawagucci et al. (2011); This study
Hatoma Knoll		21	10	Toki et al. (2016); This study
Izena Hole	JADE	0	650	Kawagucci et al. (2013); Ishibashi et al. (2014)
	HAKUREI	6.8	650	*ditto*
Yonaguni IV Knoll		13.5	1030	Konno et al. (2006); Gamo et al. (2010)
Kairei Field		0.082	52	Gamo et al. (2001)
TOTO Caldera		0.026	10	Gamo et al. (2004)

(Zhang et al., 2020), but continental water near the Kuroshio Current region, which is about 400 km away from the continent, does not seem to contain so much methane. Instead, our data suggest an origin from mud volcanoes (Figure 3C).

4.3 Marine sediments as a source of methane

While SMW effects are visible at depths shallower than 100 m from the continental shelf to the continental slope (Figures 4A–M), methane concentrations reaching 10 nM (Figures 3C, G) or 4 nM (Figure 3L) have been detected at 100–200 m. As we have mentioned, methane concentrations in seawater without anomalies decrease with depth (Figure 3U), however even on the seafloor without anomalies, methane concentrations in sediments are so much higher than in seawater that methane concentrations can increase in seawater just above the seafloor due to gas diffusion and bubble release (Reeburgh, 2007; Weber et al., 2019). On continental shelves, methane concentrations of >10 nM have been reported just above the seafloor in previous studies (Zhang et al., 2020), which likely result from methane reaching the water via sedimentary particles drifting through the seawater (Sun et al., 2018). Based on these observations, we can say that methane that was abundantly distributed in sediments disturbed by bottom currents can spread into seawater, resulting in higher methane concentrations in seawater just above seafloor. It is quite possible that methane-rich seawater just above the seafloor on the continental shelf at depths of 100–200 m formed in such a way migrates horizontally, leading to the observed methane concentration anomalies that exceed 10 nM in the water masses around 100–200 m on the continental slope.

4.4 Hydrothermal systems as a source of methane

Several different methane distributions were identified in seawater immediately above hydrothermal vents (Figures 3X, Y). Seawater sampled directly above the seafloor hydrothermal system

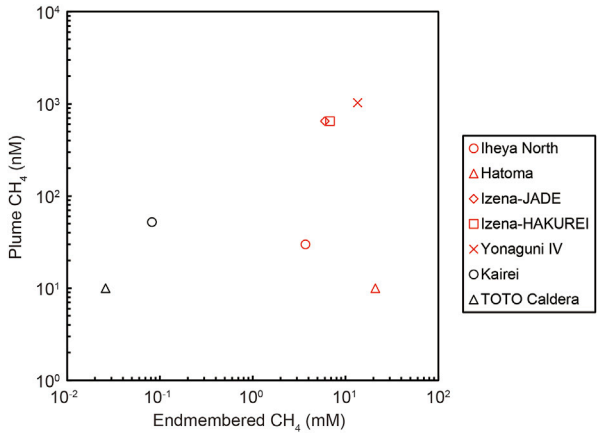

FIGURE 5
Comparison of the highest methane concentration in seawater above the hydrothermal system to the concentration of methane in the hydrothermal fluid.

shows an unparalleled methane concentration distribution (Figure 3X) that covers a range of several tens of nM, whereas a range of only a few nM with a maximum of 10 nM was observed in other areas (Figure 3Y). The submarine hydrothermal systems found at several locations in the Okinawa Trough exhibit high methane concentrations (Kawagucci, 2015). This feature is thought to be due to the geological background of the Okinawa Trough, which is classified as a sediment-covered back-arc system, from which methane from organic matter in the sediment is released when submarine hydrothermal fluids circulating through the sediment are expelled (Kawagucci, 2015). Table 2 summarizes the methane concentrations in the seafloor hydrothermal fluids of the Okinawa Trough reported to date. The maximum methane concentrations in the seawater immediately above the hydrothermally active zone are also summarized (Table 2), and for comparison, the maximum concentrations of methane detected in seawater immediately above a seafloor hydrothermal system without sediment are summarized (Table 2). A methane concentration of 3.7 mM was observed at the Iheya North Knoll,

which is marked with a red open circle (Kawagucci et al., 2011), whereas 21 mM was reported at the Hatoma Knoll, which is marked with a red open triangle (Toki et al., 2016). Two submarine hydrothermal activity zones JADE and HAKUREI, have been identified in the Izena Hole, where methane concentrations of 4.9–7.1 mM and 6.8 mM have been observed, respectively (Ishibashi et al., 2014). In addition, a value of 13.5 mM was reported for Yonaguni Knoll IV (Konno et al., 2006). By comparison, methane concentrations in the hydrothermal fluid of 82 μM were reported in a submarine hydrothermal system without sediment cover in the Kairei field at the Rodriguez Triple Junction in the Central Indian Ridge (Gamo et al., 2001) and concentrations of 2 μM were observed in the TOTO caldera at the southern end of the Mariana arc (Gamo et al., 2004). Using the Mg concentrations listed in Gamo et al. (2004), assuming that pure hydrothermal fluid contains no Mg and that all Mg is derived from seawater (Von Damm, 1995) and correcting for seawater dilution, we estimate that approximately 26 μM of hydrothermal fluids are vented from the TOTO caldera around the southern end of the Mariana arc (Gamo et al., 2004). The methane concentrations detected in the seawater immediately above the features described have been reported at ~10–1,030 nM (Table 2; Gamo et al., 2001; Gamo et al., 2004; Gamo et al., 2010; Kawagucci et al., 2010). The datasets describing these areas are shown in Figure 5.

Thus, there was an overwhelming difference in the concentration of methane in the hydrothermal fluids from the sediment-covered Okinawa Trough and that of other hydrothermal systems without sediment cover. However, regarding the methane concentrations obtained previously, little difference was observed in the methane concentrations of seawater obtained in this study (Figure 5). Furthermore, the methane concentrations in the seafloor hydrothermal fluid reported at Hatoma Knoll and Yonaguni Knoll IV were one order of magnitude higher than those at Iheya North Knoll and the Izena Hole. However, the concentration of methane in the seawater was overwhelmingly high just above Yonaguni Knoll IV and lowest at Hatoma Knoll (Figure 5). These results indicate that it is relatively difficult to quantitatively determine the methane concentration in a seafloor hydrothermal system as compared to seawater. For example, even if a Niskin water sampler is used directly above the point of a reported seafloor hydrothermal system, the proximity of the sampler to the seabed cannot be accurately determined, and the results obtained by a surface ship survey are limited by sampler sweep and the distance at which samples are obtained in the horizontal direction. Nevertheless, the methane concentrations in seawater sampled by the Niskin water sampler directly above various geological features such as the submarine hydrothermal system were found to be orders of magnitude higher those observed in seawater from other locations (Figure 3), indicating that the submarine hydrothermal system is an exceptional source of methane to the water column.

At the very least, we can be certain that there is a source of methane where water masses with methane concentrations higher than background are found. Conversely, no active sources are assumed in areas where the methane concentration is similar to background levels. If a sampler is lowered at a location where there should be a source of methane as a result of latitude and longitude but no water mass higher methane concentrations are observed, it is possible that the sampler has been swept away or that the source of methane is currently inactive. For example, anomalous methane concentrations can be detected several tens of kilometers downstream of a bottom flow stream, but not upstream, of water masses with methane concentrations higher than the background, even at a distance of only a few kilometers (Zhang et al., 2020). Indeed, it is common for no methane concentration anomalies to be detected in the seawater near undiscovered hydrothermal systems (Gamo et al., 2001; Yamanaka et al., 2015).

4.5 Mud volcanoes as a source of methane

Figure 3W shows the distribution of methane concentrations directly above a mud volcano (Ning et al., 2009), in an area where the water reaches a depth of *ca.* 1,500 m. A concentration anomaly can be observed just above the seafloor, albeit small (~1.5 nM), with background levels of methane at other depths (Figure 3W). The site marked with a brown open square (Figure 3ac) selected from the bathymetry map as a mud volcano-shaped site was associated with methane concentrations slightly above background levels approximately 100 m above the seafloor (1,200 m depth). This indicates that this site, which is located in the southern part of the Ryukyu Forearc, where no mud volcanoes have been reported, may be close to a slightly active methane venting area (Figure 1). Considering the normal places for magma formation (near an island arc, back-arc, mid-ocean ridge, or hot spot), the source of methane venting into the fore-arc would be either mud volcanoes or cold seeps.

4.6 Cold seeps as a source of methane

Seawater samples were collected over 2 years in the area directly above the cold seep site (Figure 3L: 2012, Figure 3M: 2015). In both years, very mild methane concentration anomalies (~2 nM) were found just above the seafloor surface, and once the methane concentration dropped to background levels, methane concentrations (~2.5 nM in 2015 and ~1.5 nM in 2012) were still detected in water masses a few hundred meters above the seafloor surface (Figures 3L, M). We cannot confirm whether this is an indication of methane migration via bubbles or discharge at different heights, except through direct observation of the seafloor. However, the methane concentration anomaly at around 100–200 m (~4 nM), which was observed only in 2012 at this site, may have been due to bottom currents on the continental shelf, as discussed in Section 4.3. Because this methane concentration anomaly was not observed in 2015, it can be assumed that such currents yearly, depending on the conditions just above the seafloor surface. These methane concentration anomalies (Figures 3L, M) are mild as compared to the methane concentration anomalies observed above the submarine hydrothermal systems (Figures 3X, Y) or highly active mud volcanoes (Figure 3C). This may be partly due to the relatively mild material fluxes of mainly reducing substances such as methane, hydrogen sulfide, and ammonia associated with cold-seep events as compared to mud volcanoes and submarine hydrothermal systems (Levin et al., 2016). Nevertheless, the results of this study indicate that methane can also be used to detect cold-seep activity.

4.7 Unidentified methane sources in the continental slope area

The data for water masses collected from the continental slope area are shown in green; however, because of the large number of sites, those in the north (Figures 3D–K) were plotted separately from those in the south (Figures 3N–R). Sites with relatively high methane concentrations are located farther north. The sites located to the south had relatively lower methane concentrations in comparison (<~1–3 nM); however, the overall concentrations appear more scattered than those in the background (Figures 3N–R). It is possible that the continental slope is supplying methane laterally at various depths with some phenomenon that will be discussed later (Figures 3N–R). However, this is likely not a significant source. Such a supply was observed at relatively systematic depths at the northern site, with three positive sites at 100 m (~4 nM), a large peak at approximately 150 m (~10 nM), another at 600 m (~7 nM), three at 800 m (~3 nM or ~9 nM), and one at 1,000 m (~8 nM; Figures 3D–K). The methane concentration anomalies observed at 100–200 m may indicate diffusion of methane from seafloor sediments, as discussed previously. However, the source at 1,000 m may be located on the seafloor surface, whereas the methane concentration anomalies observed around 600 m or 800 m may indicate methane on the continental slope. In the case of a submarine hydrothermal system, magma can be assumed present in the Okinawa Trough; however, the existence of magma on the continental slope area is unthinkable. As for other sources of methane supply from the seafloor, methane emissions caused by the decomposition of organic matter, such as mud volcanoes and cold seeps (Kopf, 2002), may occur even in continental slope areas. It is thought that a source of methane is present 600–1,000 m below the seafloor at around 29°N, as indicated by the green open triangles, open diamonds, and green plus marks in Figure 1.

Of these, at Site No. 2012-1 (white plus mark in green solid square; Figure 3K), seawater was also sampled in 2011 (green plus mark), at that time a small methane concentration anomaly (~2 nM) was detected at 800 m (Figure 3I). Near this site, a Chinese group recently found a cold seep (Xu et al., 2021), and bubbles emanating from the seafloor have been suggested by acoustic imagery (Chen et al., 2022). Although the detailed location has not been specified, bacterial mats and *Calyptogena* colonies have been found on the seafloor at a depth of about 900–1,000 m near 127°30′E, 29°N, and water masses with methane concentrations exceeding 20 nM have been detected in the seawater directly above the area (Zhang et al., 2020). In this study, only a maximum of approximately 8 nM was detected (Figure 3K). However, it seems certain that there was a source of methane on the seafloor in the continental slope area. Further clarification of the distribution of methane sources is required through extended seafloor observation.

4.8 Unidentified methane sources in the shelf area

Sites that are described by black open and solid squares were sampled in 2011 and 2012 by selecting an empty area on the island shelf and considering it a reference. Anomalous methane concentrations (~1.5–2.5 nM) were detected from 200 m to 600 m in 2011 (Figure 3aa), whereas anomalous methane concentrations (~1.5 nM) were detected from the surface to approximately 600 m in 2012 (Figure 3ab). This site is located on the Ryukyu Islands across the Okinawa Trough in mainland China. The Kuroshio Current flows into the sea just above the Okinawa Trough (Figure 1), and the distribution of methane in this current is at background levels (Figure 3U). The influence of continental shelf-mixed water was also observed just above the continental shelf in the yellow open circle and open triangle areas in the T-S diagram, where slightly higher methane concentrations were detected (Figures 3A, B); however, these effects are expected to be reset in the Kuroshio watershed. This suggests that the island shelf itself is the source of the methane concentration anomalies observed in the middle layers of these island shelf areas (Figures 3aa, ab). Because of the influence of domestic wastewater, rivers, and coral reefs, it is possible that groundwater that previously seeped into the subsurface may be upwelling from the coastal seafloor (Umezawa et al., 2002). Submarine groundwater discharge has been observed along the world's coasts, and it has been reported that as groundwater passes through sediments, it entrains and discharges reducing substances such as methane, hydrogen sulfide, and ammonia, which are rarely distributed in seawater (Lecher et al., 2016; Purkamo et al., 2022; Brankovits et al., 2017; Lecher, 2017; Lecher and Mackey, 2018; Sadat-Noori et al., 2018). Such an inflow of land water, such as groundwater or river water, could be observed using anomalies in the T-S diagram. However, such salinity and temperature anomalies were not visible in the T-S diagrams (Figures 2aa, ab) and the T-S profiles (Figures 4aa, ab). Therefore, groundwater and river water from the island cannot explain the anomalous methane concentrations in the middle layer that was observed at these sites. This area is not completely enclosed, but is surrounded by the Kerama Islands, Okinawajima, and Kumejima (Figure 1), and only the north, which is considered shallow water at a depth of approximately 750 m, can be considered open (Figure 1). No volcanic or hydrothermal activity was observed in the surrounding area, and the methane distribution did not seem to indicate a source on the seafloor (Figures 3aa, ab). Instead, the methane accumulates annually in this area, with concentration peaking at approximately 300–400 m, and despite the concentration differences, it appears to have peaked at the same depth in 2011 (Figure 3aa). One possible explanation is that methane seeps from the seafloor of the nearby island shelf at this depth, forming the peak. Around southern Okinawajima, an organic-rich formation called the Shimajiri Group is known to contain natural gas (Toki, 2013). The origin of methane is thought to be the Nago Formation, which is equivalent to the lower Shimanto Formation but is exposed in the Kerama Islands as the Kerama Formation (Chinen et al., 2004; Miyagi et al., 2013). In addition, faults that are associated with the marine terraces that were actively formed during the Pleistocene have been inferred along steep cliffs near the isobath at a depth of 500 m (Izumi et al., 2016), which may form pathways along which methane from beneath the seafloor can traverse. Methane accumulates in summer and is released into the atmosphere during the development of the mixed layer in winter and reset (Tsurushima et al., 1996). Its distribution varies from year to year. However, further studies are required to confirm this hypothesis.

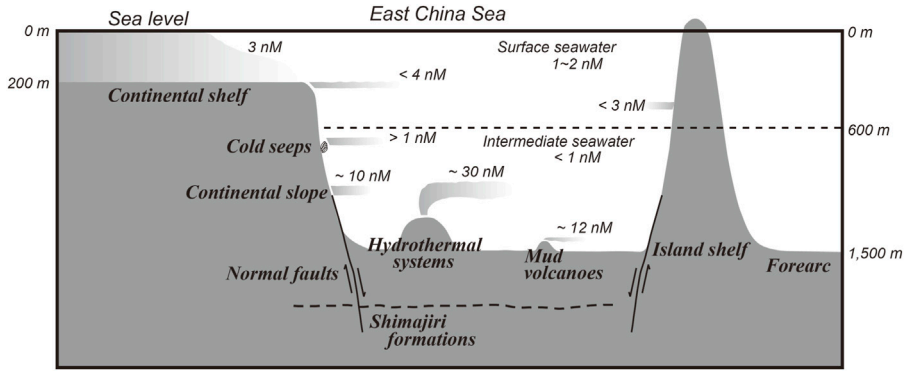

FIGURE 6
Schematic representation of representative methane sources in the East China Sea obtained in this study.

The site (black open diamond) at which the East China Sea and the Philippine Sea are connected, denoted the Tokara Gap, is located between Amami Oshima and Yakushima and has a water depth of nearly 1,100 m (Figure 1). Anomalous methane concentrations (~one to two nM) were also observed in the mid-oceanic layer at depths of 200–800 m at this site (Figure 3Z). Similar to the site denoted by the black open square, the influence of continental China is unlikely here (Figure 1). Furthermore, no influence of land-sourced water from the island is visible in the T-S diagram (Figure 2Z) and the T-S profile (Figure 4Z). However, plumes with methane concentrations of 200 nM and of 6 μM have been observed at depths of 140 m and 300–350 m, respectively, at the Tokara Islands located immediately to the west (Wen et al., 2016). The supply of these high methane concentrations can be effective, depending on the distance and direction. However, the effect is not quantifiable as the methane peak at 300 m may have been affected by high concentrations of methane spread over a distance. Because anomalous concentrations were observed to a depth of approximately 800 m, it is possible that other unknown submarine hydrothermal activities are present on the seafloor slope between the Tokara Islands and the Tokara Gap.

4.9 Overview of the sources of methane in the East China Sea

Vertical sampling of seawater was conducted intermittently over the East China Sea in early June from 2011 to 2015. The combination of temperature and salinity indicates that different water masses are distributed in each geographical area, such as the Kuroshio, continental slope, and continental shelf regions, which can be explained by water masses mixing with continental shelf mixed water, which comprises pure seawater and river water from the continent. On the other hand, an additional feature observed in the methane concentration indicates the presence of a geological singularity (Figure 6). Mild anomalies in the methane concentration were observed in the water masses around the continental shelf area, suggesting the influence of water with high organic matter and methane content derived from the diffusion of methane from seafloor sediments. Seawater sampled just above the mud volcano also showed larger methane concentrations, which probably depend on the activity level and distance to which the water sampler was swept from the volcano. The identification of the world's first methane concentration anomaly indicating the presence of a mud volcano that is not associated with the southern Ryukyu Islands created a stir for future research on new mud volcanoes.

Anomalous methane concentrations were observed directly above the submarine hydrothermal system at levels not observed in other areas, indicating the high potential of this area as a source of methane. Anomalous methane concentrations were also observed directly above the cold-seep site, but not the submarine hydrothermal system. During the 2 years over which samples were taken from the cold seep site, high methane concentrations observed just above the seafloor on both occasions indicate that the cold seep was definitely discharging methane. In addition, anomalous methane concentrations were often observed at 100–200 m in the vertical profiles collected from continental slope areas, including a cold-seep site, suggesting that diffusion from submarine sediments on the continental shelf was probably the source of the methane. The vertical profiles of seawater sampled from the continental slope appear to show greater methane concentration scatter than other areas of the ocean as compared to the background. This suggests that methane is supplied from continental slopes at various depths, and may be the cause of the variation in concentration. This is particularly true for the continental slope around 29°N, where methane concentrations are high, suggesting that the continental slope itself may provide other sources of methane such as cold seeps and mud volcanoes, which are not related to igneous activity. In addition, slight anomalies in the methane concentrations were detected mid-level in the shelf area of the Ryukyu Islands. Because methane seeps from the surrounding seafloor may occur, it is necessary to search for seafloor phenomena such as cold seeps, mud volcanoes, or submarine hydrothermal activity that could be sources of methane in the continental slope area, southern Ryukyu forearc, and the Ryukyu Islands shelf area.

5 Conclusion

Our study of methane distribution in seawater around the Ryukyu Arc reveals the following. Terrestrial water from continental China is a relatively mild source of methane to seawater (<4 nM), while more methane appears to be supplied by mud volcanoes (~12 nM). In addition, submarine hydrothermal systems are a uniquely large source of methane (~30 nM). The continental slope appears to be a source of methane mainly north of 29°N (~10 nM). High concentrations (<3 nM) of methane water masses have also been detected on the island shelf and in forearc region, and it appears that there are still undiscovered sources of methane on the island shelf and in forearc region.

Data availability statement

The original contributions presented in the study are included in the article/Supplementary Material, further inquiries can be directed to the corresponding author.

Author contributions

TT took on all the roles. Others assisted with sampling, performed analysis, and analyzed data.

Funding

This work was supported by the "Okinawa Research Core for Highly Innovative Discipline Science (ORCHIDS)" project at the Faculty of Science, University of the Ryukyus during 2017–2021, JSPS KAKENHI Grant Numbers 18H03733, 20H04315, and 23K11391, the Research Institute of Science and Technology for Society (RISTEX), Solution-Driven Co-creative R&D Program for SDGs (SOLVE for SDGs) the "Development of watershed governance based on participation and consensus for sustainable water resource use on subtropical islands" (funding agency: Japan Science and Technology Agency; JST) during 2019–2023, and the Research Institute for Humanity and Nature (RIHN: a constituent member of NIHU) Project "Adaptive Governance of Multiple Resources based on Land-Sea Linkages of the Water Cycle: Application to Coral Reef Island Systems (LINKAGE; No. 14200145)".

Acknowledgments

This paper was developed as part of the graduation works produced by HC, TS, and YY; our heartfelt gratitude goes to every professor and staff member at the University of Ryukyus who were associated with examining this work. We are also grateful to the Captain and crew of the T/V Nagasaki for sampling the seawater. We would like to thank Editage (www.editage.com) for English language editing. We would like to express our deep gratitude to Professor MK, who edited the paper patiently from the poor first draft, and to the three reviewers (Professor SA, NS, and Professor SL).

Conflict of interest

The authors declare that the research was conducted in the absence of any commercial or financial relationships that could be construed as a potential conflict of interest.

Publisher's note

Supplementary material

The Supplementary Material for this article can be found online at: https://www.frontiersin.org/articles/10.3389/feart.2023.1174504/full#supplementary-material

References

Bange, H. W. (2006). Nitrous oxide and methane in European coastal waters. *Estuar. Coast. Shelf Sci.* 70, 361–374. doi:10.1016/j.ecss.2006.05.042

Bange, H. W., Bartell, U. H., Rapsomanikis, S., and Andreae, M. O. (1994). Methane in the Baltic and North Seas and a reassessment of the marine emissions of methane. *Glob. Biogeochem. Cycles.* 8, 465–480. doi:10.1029/94GB02181

Brankovits, D., Pohlman, J. W., Niemann, H., Leigh, M. B., Leewis, M. C., Becker, K. W., et al. (2017). Methane- and dissolved organic carbon-fueled microbial loop supports a tropical subterranean estuary ecosystem. *Nat. Commun.* 8, 1835. doi:10.1038/s41467-017-01776-x

Cao, H., Sun, Z., Wu, N., Liu, W., Liu, C., Jiang, Z., et al. (2020). Mineralogical and geochemical records of seafloor cold seepage history in the northern Okinawa Trough, East China Sea. *Deep Sea Res. I.* 155, 103165. doi:10.1016/j.dsr.2019.103165

Chen, Y., Xu, C., Wu, N., Sun, Z., Liu, C., Zhen, Y., et al. (2022). Diversity of anaerobic methane oxidizers in the cold seep sediments of the Okinawa Trough. *Front. Microbiol.* 13, 819187. doi:10.3389/fmicb.2022.819187

Chinen, M., Shinjo, R., and Kato, Y. (2004). Occurrence and geochemistry of *in-situ* greenstones from the Shimanto belt in the Ryukyu islands. *Ganseki Kobutsu Kagaku Mineral. Petrol. Sci.* 33, 208–220. doi:10.2465/gkk.33.208

Gamo, T., Chiba, H., Yamanaka, T., Okudaira, T., Hashimoto, J., Tsuchida, S., et al. (2001). Chemical characteristics of newly discovered black smoker fluids and associated hydrothermal plumes at the Rodriguez Triple Junction, Central Indian Ridge. *Earth Planet. Sci. Lett.* 193, 371–379. doi:10.1016/S0012-821X(01)00511-8

Gamo, T., Masuda, H., Yamanaka, T., Okamura, K., Ishibashi, J., Nakayama, E., et al. (2004). Discovery of a new hydrothermal venting site in the southernmost Mariana Arc: Al-rich hydrothermal plumes and white smoker activity associated with biogenic methane. *Geochem J.* 38, 527–534. doi:10.2343/geochemj.38.527

Gamo, T., Tsunogai, U., Ichibayashi, S., Chiba, H., Obata, H., Oomori, T., et al. (2010). Microbial carbon isotope fractionation to produce extraordinarily heavy methane in aging hydrothermal plumes over the southwestern Okinawa Trough. *Geochem. J.* 44, 477–487. doi:10.2343/geochemj.1.0097

Holmes, M. E., Sansone, F. J., Rust, T. M., and Popp, B. N. (2000). Methane production, consumption, and air-sea exchange in the open ocean: an Evaluation based on carbon isotopic ratios. *Glob. Biogeochem. Cycles.* 14, 1–10. doi:10.1029/1999GB001209

Ishibashi, J., Noguchi, T., Toki, T., Miyabe, S., Yamagami, S., Onishi, Y., et al. (2014). Diversity of fluid geochemistry affected by processes during fluid upwelling in active

hydrothermal fields in the Izena Hole, the middle Okinawa Trough back-arc basin. *Geochem. J.* 48, 357–369. doi:10.2343/geochemj.2.0311

Izumi, N., Nishizawa, A., Horiuchi, D., Kido, Y., Goto, H., and Nakata, T. (2016). 3D bathymetric image of Nansei-shoto Trench and its vicinity (in Japanese with English abstract). *Rep. Hydrogr. Oceanogr. Res.*, 133–149.

Kawagucci, S. (2015). "Fluid geochemistry of high-temperature hydrothermal fields in the Okinawa Trough: how and where TAIGA of methane is generated," in *Subseafloor biosphere linked to global hydrothermal systems; TAIGA concept*. Editors K. Okino, J. Ishibashi, and M. Sunamura (Tokyo Heidelberg New York Dordrecht London: Springer), 387–403.

Kawagucci, S., Chiba, H., Ishibashi, J., Yamanaka, T., Toki, T., Muramatsu, Y., et al. (2011). Hydrothermal fluid geochemistry at the Iheya North field in the mid-Okinawa Trough: implication for origin of methane in subseafloor fluid circulation systems. *Geochem. J.* 45, 109–124. doi:10.2343/geochemj.1.0105

Kawagucci, S., Shirai, K., Lan, T. F., Takahata, N., Tsunogai, U., Sano, Y., et al. (2010). Gas geochemical characteristics of hydrothermal plumes at the HAKUREI and JADE vent sites, the Izena Cauldron, Okinawa Trough. *Geochem. J.* 44, 507–518. doi:10.2343/geochemj.1.0100

Kawagucci, S., Ueno, Y., Takai, K., Toki, T., Ito, M., Inoue, K., et al. (2013). Geochemical origin of hydrothermal fluid methane in sediment-associated fields and its relevance to the geographical distribution of whole hydrothermal circulation. *Chem. Geol.* 339, 213–225. doi:10.1016/j.chemgeo.2012.05.003

Konno, U., Tsunogai, U., Nakagawa, F., Nakaseama, M., Ishibashi, J., Nunoura, T., et al. (2006). Liquid CO_2 venting on seafloor: Yonaguni IV Knoll hydrothermal system, Okinawa Trough. *Geophys. Res. Lett.* 33, L16607. doi:10.1029/2006GL026115

Kopf, A. J. (2002). Significance of mud volcanism. *Rev. Geophys.* 40, 1005. doi:10.1029/2000rg000093

Kuhara, T., Kano, Y., Yoshikoshi, K., and Hashimoto, J. (2014). Shell morphology, anatomy and gill histology of the deep-sea bivalve *Elliptio lucina ingens* and molecular phylogenetic reconstruction of the chemosynthetic family Lucinidae. *Venus J. Malacol. Soc. Jpn.* 72, 13–27. doi:10.18941/venus.72.1-4_13

Lecher, A. L. (2017). Groundwater discharge in the Arctic: a review of studies and implications for biogeochemistry. *Hydrology* 4, 41. doi:10.3390/hydrology4030041

Lecher, A. L., Kessler, J., Sparrow, K., Garcia-Tigreros Kodovska, F., Dimova, N., Murray, J., et al. (2016). Methane transport through submarine groundwater discharge to the North Pacific and Arctic Ocean at two Alaskan sites. *Limnol. Oceanogr.* 61, S344–S355. doi:10.1002/lno.10118

Lecher, A. L., and Mackey, K. R. M. (2018). Synthesizing the effects of submarine groundwater discharge on marine biota. *Hydrology* 5, 60. doi:10.3390/hydrology5040060

Levin, L. A., Baco, A. R., Bowden, D. A., Colaco, A., Cordes, E. E., Cunha, M. R., et al. (2016). Hydrothermal vents and methane seeps: rethinking the sphere of influence. *Front. Mar. Sci.* 3. doi:10.3389/fmars.2016.00072

Li, Q., Cai, F., Liang, J., Shao, H., Dong, G., Wang, F., et al. (2015). Geochemical constraints on the methane seep activity in western slope of the middle Okinawa Trough, the East China Sea. *Sci. China Earth Sci.* 58, 986–995. doi:10.1007/s11430-014-5034-x

Miyagi, N., Baba, S., and Shinjo, R. (2013). Whole-rock chemical composition of the pre-Neogene basement rocks and detritus garnet composition in the Okinawa-jima and neighbor islands. *Jour. Geol. Soc. Jpn.* 119, 665–678. doi:10.5575/geosoc.2013.0045

Monma, H., Iwase, R., Mitsuzawa, K., Kaiho, Y., Fujiwara, Y., Amitani, Y., et al. (1996). Deep tow survey in Nanseishoto Region (K95-07-NSS) (In Japanese with English abstract). *JAMSTEC Journal of Deep Sea Research* 12, 195–210.

Ning, X., Shiguo, W., Buqing, S., Bing, L., Liangqing, X., Xiujuan, W., et al. (2009). Gas hydrate associated with mud diapirs in southern Okinawa Trough. *Mar. Petrol. Geol.* 26, 1413–1418. doi:10.1016/j.marpetgeo.2008.10.001

Peng, X., Guo, Z., Chen, S., Sun, Z., Xu, H., Ta, K., et al. (2017). Formation of carbonate pipes in the northern Okinawa Trough linked to strong sulfate exhaustion and iron supply. *Geochim. Cosmochim. Acta.* 205, 1–13. doi:10.1016/j.gca.2017.02.010

Purkamo, L., Von Ahn, C. M. E., Jilbert, T., Muniruzzaman, M., Bange, H. W., Jenner, A.-K., et al. (2022). Impact of submarine groundwater discharge on biogeochemistry and microbial communities in pockmarks. *Geochim. Cosmochim. Acta.* 334, 14–44. doi:10.1016/j.gca.2022.06.040

Reeburgh, W. S. (2007). Oceanic methane biogeochemistry. *Chem. Rev.* 107, 486–513. doi:10.1021/cr050362v

Sadat-Noori, M., Tait, D. R., Maher, D. T., Holloway, C., and Santos, I. R. (2018). Greenhouse gases and submarine groundwater discharge in a Sydney Harbour embayment (Australia). *Estuar. Coast. Shelf Sci.* 207, 499–509. doi:10.1016/j.ecss.2017.05.020

Shukla, R., Slade, A., Khourdajie, A., Van Diemen, R., Mccollum, D., Pathak, M., et al. (2022). in *Mitigation of climate change. Contribution of working group III to the sixth assessment report of the intergovernmental panel on climate change*. Editor P. R. Shuka (New York, NY: Cambridge, UK). IPCC (2022). Clim. Change.

Sun, M.-S., Zhang, G.-L., Ma, X., Cao, X.-P., Mao, X.-Y., Li, J., et al. (2018). Dissolved methane in the East China Sea: distribution, seasonal variation and emission. *Mar. Chem.* 202, 12–26. doi:10.1016/j.marchem.2018.03.001

Sun, Z., Wei, H., Zhang, X., Shang, L., Yin, X., Sun, Y., et al. (2015). A unique Fe-rich carbonate chimney associated with cold seeps in the northern Okinawa Trough, East China Sea. *Deep Sea Res. I.* 95, 37–53. doi:10.1016/j.dsr.2014.10.005

Sun, Z., Wu, N., Cao, H., Xu, C., Liu, L., Yin, X., et al. (2019). Hydrothermal metal supplies enhance the benthic methane filter in oceans: an example from the Okinawa Trough. *Chem. Geol.* 525, 190–209. doi:10.1016/j.chemgeo.2019.07.025

Toki, T. (2013). Distribution of crustal fluid mainly composed by methane around the Ryukyu Islands and its relationship with geological settings (in Japanese with English abstract). *Chikyukagaku (Geochem.)* 47, 53–69. doi:10.14934/chikyukagaku.47.53

Toki, T., Itoh, M., Iwata, D., Ohshima, S., Shinjo, R., Ishibashi, J., et al. (2016). Geochemical characteristics of hydrothermal fluids at hatoma Knoll in the southern Okinawa Trough. *Geochem. J.* 50, 493–525. doi:10.2343/geochemj.2.0449

Tsurushima, N., Watanabe, S., and Tsunogai, S. (1996). Methane in the East China sea water. *J. Oceanogr.* 52, 221–233. doi:10.1007/BF02235671

Umezawa, Y., Miyajima, T., Kayanne, H., and Koike, I. (2002). Significance of groundwater nitrogen discharge into coral reefs at Ishigaki Island, southwest of Japan. *Coral Reefs* 21, 346–356. doi:10.1007/s00338-002-0254-5

Von Damm, K. L. (1995). "Controls on the chemistry and temporal variability of seafloor hydrothermal fluids," in *Seafloor hydrothermal systems: physical, chemical, biological, andgeological interactions*. Editors S. E. Humphris, R. A. Zierenberg, L. S. Mullineaux, and R. E. Thomson (Washington DC: American Geophysical Union), 222–247.

Watanabe, S., Higashitani, N., Tsurushima, N., and Tsunogai, S. (1995). Methane in the western north pacific. *J. Oceanogr.* 51, 39–60. doi:10.1007/BF02235935

Weber, T., Wiseman, N. A., and Kock, A. (2019). Global ocean methane emissions dominated by shallow coastal waters. *Nat. Commun.* 10, 4584. doi:10.1038/s41467-019-12541-7

Wen, H. Y., Sano, Y., Takahata, N., Tomonaga, Y., Ishida, A., Tanaka, K., et al. (2016). Helium and methane sources and fluxes of shallow submarine hydrothermal plumes near the Tokara Islands, Southern Japan. *South. Jpn. Sci. Rep.* 6, 34126. doi:10.1038/srep34126

Xing, J., Jiang, X., and Li, D. (2016). Seismic study of the mud diapir structures in the Okinawa Trough. *Geol. J.* 51, 203–208. doi:10.1002/gj.2824

Xu, C., Wu, N., Sun, Z., Zhang, X., Geng, W., Cao, H., et al. (2021). Assessing methane cycling in the seep sediments of the mid-Okinawa Trough: insights from pore-water geochemistry and numerical modeling. *Ore Geol. Rev.* 129, 103909. doi:10.1016/j.oregeorev.2020.103909

Yamanaka, T., Nagashio, H., Nishio, R., Kondo, K., Noguchi, T., Okamura, K., et al. (2015). "The Tarama Knoll: geochemical and biological profiles of hydrothermal activity," in *Subseafloor biosphere linked to global hydrothermal systems; TAIGA concept*. Editors K. Okino, J. Ishibashi, and M. Sunamura (Tokyo Heidelberg New York Dordrecht London: Springer), 497–504.

Yin, P., Berné, S., Vagner, P., Loubrieu, B., and Liu, Z. (2003). Mud volcanoes at the shelf margin of the East China Sea. *Mar. Geol.* 194, 135–149. doi:10.1016/S0025-3227(02)00678-3

Zhang, G., Zhang, J., Ren, J., Li, J., and Liu, S. (2008). Distributions and sea-to-air fluxes of methane and nitrous oxide in the north East China Sea in summer. *Mar. Chem.* 110, 42–55. doi:10.1016/j.marchem.2008.02.005

Zhang, X., Sun, Z., Wang, L., Zhang, X., Zhai, B., Xu, C., et al. (2020). Distribution and discharge of dissolved methane in the middle Okinawa Trough, East China sea. *Front. Earth Sci.* 8. doi:10.3389/feart.2020.00333